RSC Advances

ROYAL SOCIETY OF CHEMISTRY

www.rsc.org/advances

Cite this: DOI: 10.1039/c0xx00000x

www.rsc.org/xxxxxx

ARTICLE TYPE

Electric Field Effect on the Ground State Proton Transfer in the H-bonded HBDI Complex: An Implication of Green Fluorescent Protein

Baotao Kang,[a] Hongguang Liu,[a] Du-Jeon Jang,[b] Jin Yong Lee [a] *

Received (in XXX, XXX) Xth XXXXXXXXX 20XX, Accepted Xth XXXXXXXXX 20XX

DOI: 10.1039/b000000x

In this paper, first-principle calculations were performed regarding the electric field effect on the ground state proton transfer (GSPT) in the H-bonded p-hydroxybenzylideneimidazolidinone (HBDI) network that represents the active site of the green fluorescent protein (GFP). Potential energy surfaces (PESs) in the absence or presence of electric fields were obtained by DFT calculations with CAM-B3LYP functional. Surprisingly, it was found that the magnitude of equilibrium constant (***K***) under the electric fields can be closely fitted to a linear relationship. The concerted and asynchronous proton transfer mechanism in field free condition can be altered by the electric field. Moreover, electric field parallel to the ***x*** axis (***Fx***) has the strongest effect on the absorption energy of both the neutral and anionic HBDI complexes. Our results demonstrate the electric field can be used for the rational design of GFP mutants with desirable properties.

Introduction

The green fluorescent protein (GFP) from jellyfish is no doubt a shining star due to its unique photophysical properties that has been widely used for *in vivo* imaging of intact living cells and organisms. [1-3] To highlight the importance of this finding, the 2008 Nobel Prize in Chemistry was awarded to Shiomura, Chalfie and Tsien for their discovery and development of GFP.[4] Nonetheless, the *wt*-GFP does have some disadvantages, such as weak fluorescence signals and broad absorption spectrum. Thus, extensive efforts have been undertaken to engineer different mutants of GFP with useful photophysical characteristics.[5] One way is to properly functionalize the chromophore. The chromophore of *wt*-GFP, *p*-hydroxybenzylideneimidazolidinone (HBDI as illustrated in Scheme 1), has two absorption bands at 398 nm (neutral form)[6] and 475 nm (anionic form).[7] The HBDI can be functionalized to hydroxybenzilidene-1-methyl-2-penta-1,3dien-1-yl-imidazolidinone (HBMPDI) as the chromophore for DsRFP [8] or 2-acetyl-4-p-hydroxybenzylidene-1-methyl- 5-imidazolone (AHBMI) as the chromophore for FP595.[9] The other way is to properly manipulate the surrounding environment of GFP. The HBDI is rigidly encapsulated in the GFP cavity and surrounded by an enormous number of both charged and polar residues.[10, 11] Besides *p*H[12, 13] and temperature[14, 15], these residues provide resources for rational strategy to modify and expand the fluorescence behavior of GFP. Residues near the chromophore would have direct steric effects on the absorption and/or emission spectra.[11, 16] Another important environment factor, electric field, induced by residues comes into our vision.

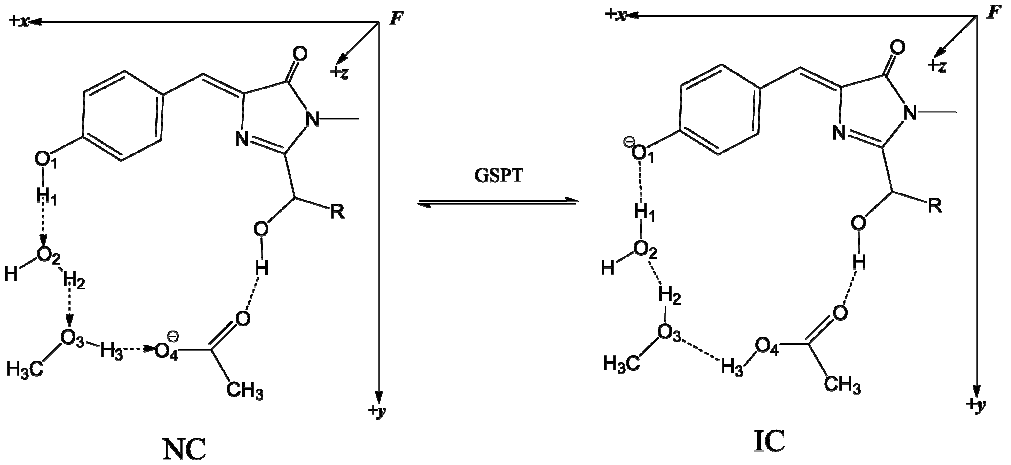

Scheme 1. Illustration of the GSPT process of the selected H-bonded HBDI complex.

It is noteworthy that the electric field, which has reported to significantly influence on nearly every aspect of protein functions,[17-19] can be created by the charged and polar residues inside the GFP cavity, with strength up to 80 MV/cm.[20-22] Conceivably, such strong electric field is one of the key elements that should not be ignored when probing physical or chemical properties related with GFP. However, still not many research works have adequately engaged in this issue and aroused concerns it deserves. The electric field can be employed to decrease or even turn off the fluorescence of intact GFP mutants as a result of the field-induced enhancement in the rate of non-radiative process from the fluorescent state. [23, 24] When the isolated neutral HBDI is placed on poly (methyl methacrylate) (PMMA) film, electric fields can increase the fluorescence lifetime arising from the de-enhancement of the non-radiative process caused by the steric hindrance of the polymer film.[25] In the meantime, it was found that electric field can affect the absorption spectra of HBDI. However, electric field with strength of only 1 MV/cm was applied without any information about field orientation, which could not adequately simulate the electrostatic environment inside the GFP cavity. Moreover, theoretical investigation has been performed to study the electric field effects on the absorption of anionic form of DsRed chromophore.[26] Electric field applied along certain orientations can account for fairly large shift in the absorption energy as reflected by the HOMO-LUMO gap with field strength up to 50MV/cm. Nevertheless, electric field effects on substances can be classified into two categories: in low fields, roughly below 1 MV/cm, atoms and molecules become polarized and such effects is called physical; in larger fields, chemical effects come into play because orbitals can be distorted.[27] In this regard, time-dependent DFT (TDDFT) should be more appropriate to describe the photochemical properties under such strong electric field. Hence, electric field effects on the absorption energies were taken into account for both the neutral and anionic forms by TDDFT calculations.

Besides, unstable molecules may be stabilized by strong electric field, which could induce new pathways in chemical reactions. Electric fields have been reported to significantly impact the shapes of PESs for proton transfer reactions.[28, 29] For example, electric fields show potently influence the barrier and rate constant of the double proton transfer in the formic acid dimer (a model for the base pair in DNA)[30]. An electric field with strength of 51.40 MV/ cm can lower the reaction barrier by ~30%. Hence, it is reasonable to expect the electric field should influence the GSPT process in GFP. However, to our knowledge, this issue is still up in the air. For the conversion between neutral to anionic chromophore in GFP, a mechanism was proposed which is well-known as a three state isomerization model with an intermediate state.[31] It was confirmed that the change from neutral to intermediate is simply a change of protonation state, while the change from I to A is a sterically demanding conformational change involving the residues.[10, 32, 33] Hereof, we mainly focus on the GSPT between neutral and intermediate state. Electric fields were employed along each axial direction and the corresponding PES was investigated along the proton transfer coordinates. The proton motions were probed to see how the GSPT mechanism evolves under electric fields. Our results reveal that electric field parallel to every axis has noticeable effects on the GSPT process, while field parallel to $\boldsymbol{x}$ axis can counts for large shift in absorption energy. Since the direction and strength of electric field are controllable by altering the position of charged or polar amino acid residues,[34, 35] the present work will pave theoretical basis for the rational design of new variants of GFP with desirable properties

Computational Method

Considering the complexity of real GFP, quantum mechanical methods turn to be a feasible alternative to experiment in understanding the electric field effects on proton transfer in GFP. The HBDI is surrounded by hundreds of residues in GFP cavity, whereas only the residues nearby are correlated with the proton abstraction. Herein, the active site including residue Water 22, Ser 205 and Glu 222 that are responsible for GSPT was selected. The HBDI in systematical arrangement with water, methanol (stands for Ser205) and acetate (stands for Glu 222) were assembled to recreate the H-bonding network (as shown in Scheme 1), which has been widely used as the model to study proton transfer in GFP.[36-39] To achieve our goal, DFT calculations, which have been well accepted to optimize the ground state structures of GFP,[40] were carried out by a suite of Gaussian 09 programs.[41] Since a partial charge transfer (CT) can take place during photoexcitation of FPs,[42] to better engage in this problem, we employed a DFT method with long-range corrected B3LYP by using the Coulomb-attenuating method (CAM-B3LYP),[43] which has been proved to perform well in describing H-bonded chains[44] and CT state.[45-47] For the electric field condition, a finite dipole field with different strengths was applied. All the geometries were fully optimized by CAM-B3LYP/6-31+G*, and the corresponding PESs were investigated. The intrinsic reaction coordinate (IRC) calculations[48] were performed to confirm whether the transition state connects to the reactant and product. Frequency calculations were employed to analyze the vibrational mode, as well as to get the zero point energy (ZPE) correction. Unless mentioned otherwise, the energy differences and energy barriers reported here are ZPE corrected Gibbs free energies.

Once the activation barrier was obtained, the reaction rate constant can be approximately estimated by conventional transition state theory (CTST),[49] which is the most widely used for calculating chemical reaction rate constants (k). The CTST rate constant expression is written as:

$$k(\mathrm{T}) = \frac{Q_{TS}}{Q_{RC}} \frac{k_B T}{h} \exp(-\frac{\Delta G^{\ddagger}}{RT})$$

where Q_{TS}, Q_{RC}, k_B, T, h, $\Delta G^{\ddagger}$ and R are the partition function of transition state, partition function of reactant complex, Boltzmann constant, absolute temperature, Planck's constant, Gibbs activation energy (G_{TS}-G_{RC}) and gas constant.

Results and Discussions

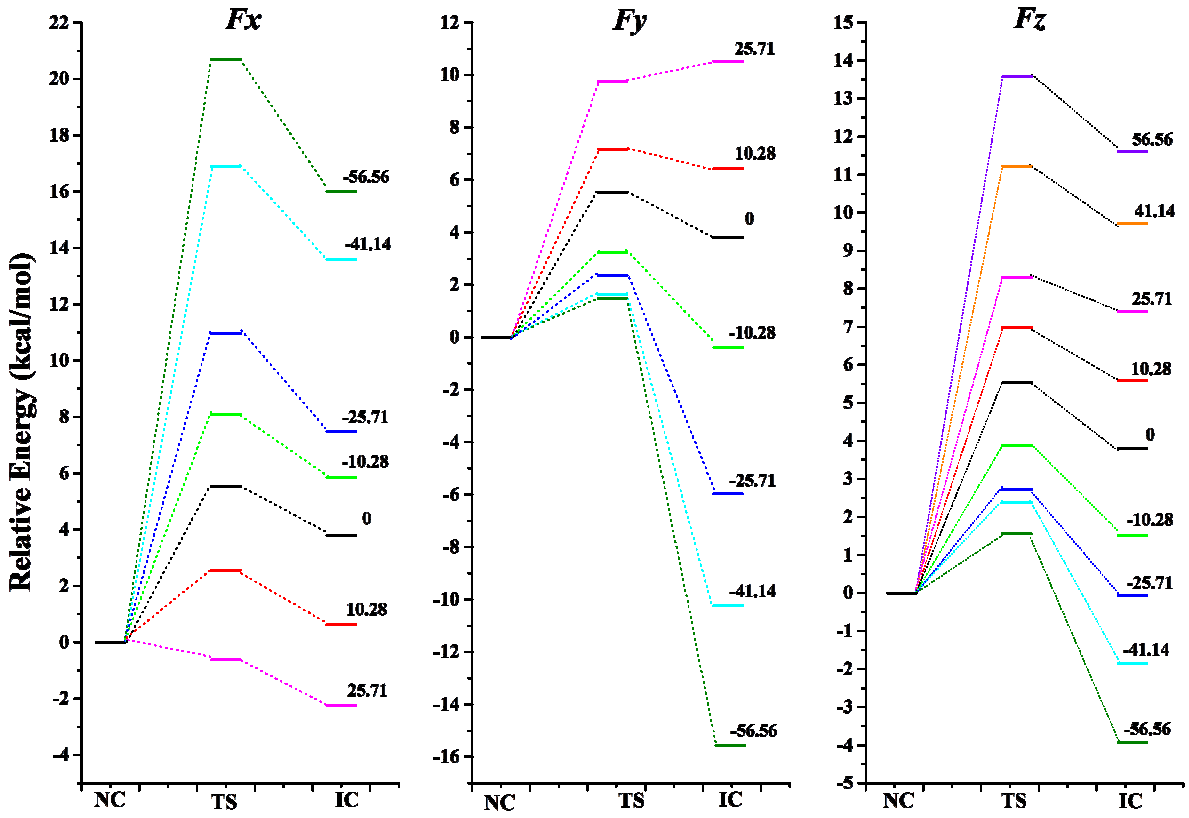

Figure 1. Potential energy surfaces along the GSPT process under the influence of electric fields.

The GSPT process concerted here involves a triple proton transfer as illustrated in Scheme 1. In the electric field free condition, the PES was obtained along the proton transfer coordinates by CAM-B3LYP. From the PES, two local minima were denoted by neutral complex (NC) and intermediate complex (IC) according to the protonation state of HBDI, and the transition state was denoted by TS. Through frequency calculations, it was confirmed that NC and IC are real local minima without any imaginary frequency, and TS is a saddle point with the only imaginary frequency of 418 icm^{-1}. The connection of TS to NC and IC was verified by IRC calculation as well. For the forward process from NC to IC, the Gibbs free energy barrier ($\Delta G^{\ddagger}$) was calculated to be 5.52 kcal/mol, and the relative stability between NC and IC (ΔE) is 3.80 kcal/mol where NC is more stable in energy than IC. Our results are in line with the experimental results quite well (5.53 kcal and 1.62 kcal/mol respectively).[50] Considering the smaller energy barrier and relative stability, both the forward and backward reactions can take place, while NC is the dominating conformer. In the meantime, the GSPT process, as stated in introduction, deeply depends on the surrounding environment such as pH[12, 13] and temperature[14, 15] as well the electric field studied here.

Table 1. Energy difference (ΔE/kcal mol^{-1}), energy barrier ($\Delta G^{\ddagger}$/kcal mol^{-1}), forward reaction rate (k_1/s^{-1}) and backward reaction rate (k_2/s^{-1}) under electric fields.

F		-56.56	-41.14	-25.71	-10.28	0	10.28	25.71	41.14	56.56
x	ΔE	15.99	13.58	7.49	5.85	3.80	0.62	-2.24	NA	NA
	$\Delta G^{\ddagger}$	20.69	16.90	10.96	8.09	5.52	2.55	-0.62	NA	NA
	k_1	2.8×10^{-2}	2.4×10^{3}	6.9×10^{7}	2.9×10^{9}	4.5×10^{11}	1.1×10^{13}	1.7×10^{15}	NA	NA
	k_2	7.9×10^{9}	8.1×10^{12}	1.1×10^{13}	6.7×10^{13}	8.7×10^{13}	2.0×10^{13}	1.3×10^{13}	NA	NA
y	ΔE	-15.56	-10.23	-5.97	-0.39	3.80	6.44	10.52	NA	NA
	$\Delta G^{\ddagger}$	1.47	1.63	2.35	3.24	5.52	7.17	9.74	NA	NA
	k_1	1.5×10^{14}	7.9×10^{14}	1.0×10^{13}	7.1×10^{12}	4.5×10^{11}	4.3×10^{10}	3.6×10^{8}	NA	NA
	k_2	1.2×10^{2}	9.2×10^{6}	5.5×10^{8}	6.5×10^{12}	8.7×10^{13}	8.2×10^{13}	4.8×10^{14}	NA	NA
z	ΔE	-3.92	-1.86	-0.07	1.52	3.80	5.57	7.41	9.71	11.61
	$\Delta G^{\ddagger}$	1.55	2.38	2.73	3.88	5.52	6.98	8.30	11.22	13.57
	k_1	1.6×10^{14}	8.2×10^{12}	1.1×10^{13}	1.1×10^{12}	4.5×10^{11}	4.4×10^{9}	4.5×10^{9}	1.3×10^{7}	5.9×10^{4}
	k_2	2.3×10^{10}	1.7×10^{11}	9.9×10^{12}	1.9×10^{13}	8.7×10^{13}	7.0×10^{13}	2.6×10^{15}	6.0×10^{14}	4.1×10^{13}

Temperature: 298.15K, Pressure: 1 atm

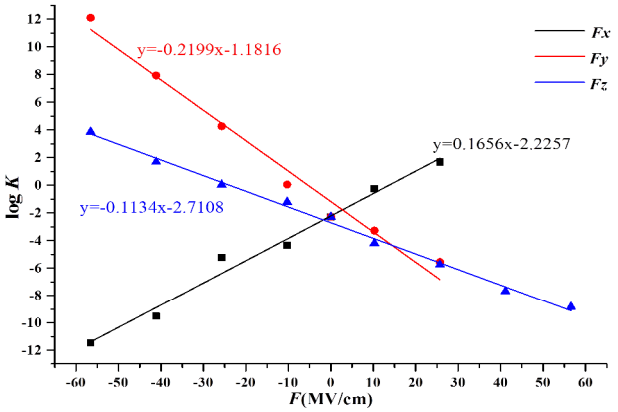

Figure 2. Equilibrium constants vs. electric fields.

As is well known, electric field has significant effect on nearly every aspect of FPs. Nevertheless, this issue is not easily approached by experiments. Thus, quantum mechanical (QM) stimulations turn to be a viable alternative to experiments in understanding the property changes under electric field at the molecular level. Electric fields parallel to three orthogonal axial orientations (***Fx***, ***Fy*** and ***Fz***) were explored as depicted in Scheme 1. The positive direction of ***Fx*** was defined as starting from imidazolium towards phenol, while the positive direction of ***Fz*** is perpendicular to the plane of HBDI and upwards. All the structures were fully re-optimized including the electric fields, and the corresponding PESs were plotted in Figure 1, the detailed information was listed in Table 1 and optimized structures of NC and IC are available in Figure S1. For the positive ***Fx*** and ***Fy***, it is worthy to note that only field strengths to 25.71 MV/cm are available, since the H-bonding network is broken under stronger field (41.14 MV/cm and 56.56 MV/cm). Taking the complexity of real GFP environment into consideration, it requires further

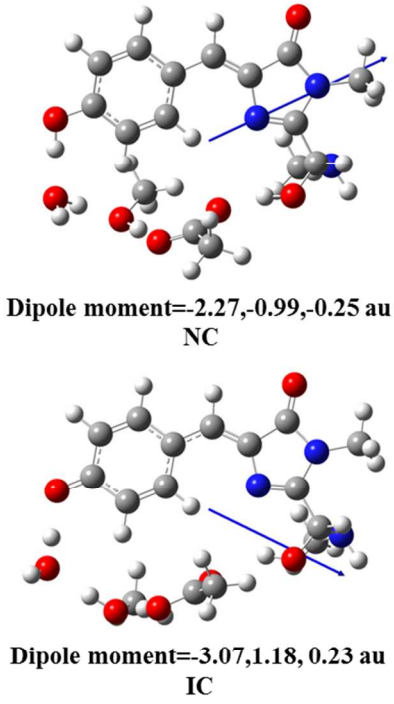

Figure 3. Calculated dipole moments of NC and IC (White: hydrogen; Gray: carbon; Red: oxygen; Blue: nitrogen).

confirmation by experimental as well as theoretical efforts. Proposing this H-bond breaking under strong electric field to be true in real GFP environments, it may provide some new proton transfer pathways or steric conformation changes. Considering the environment around the substrate, the mutation of nonpolar residue such as Phe 165 can change internal electric field, hence

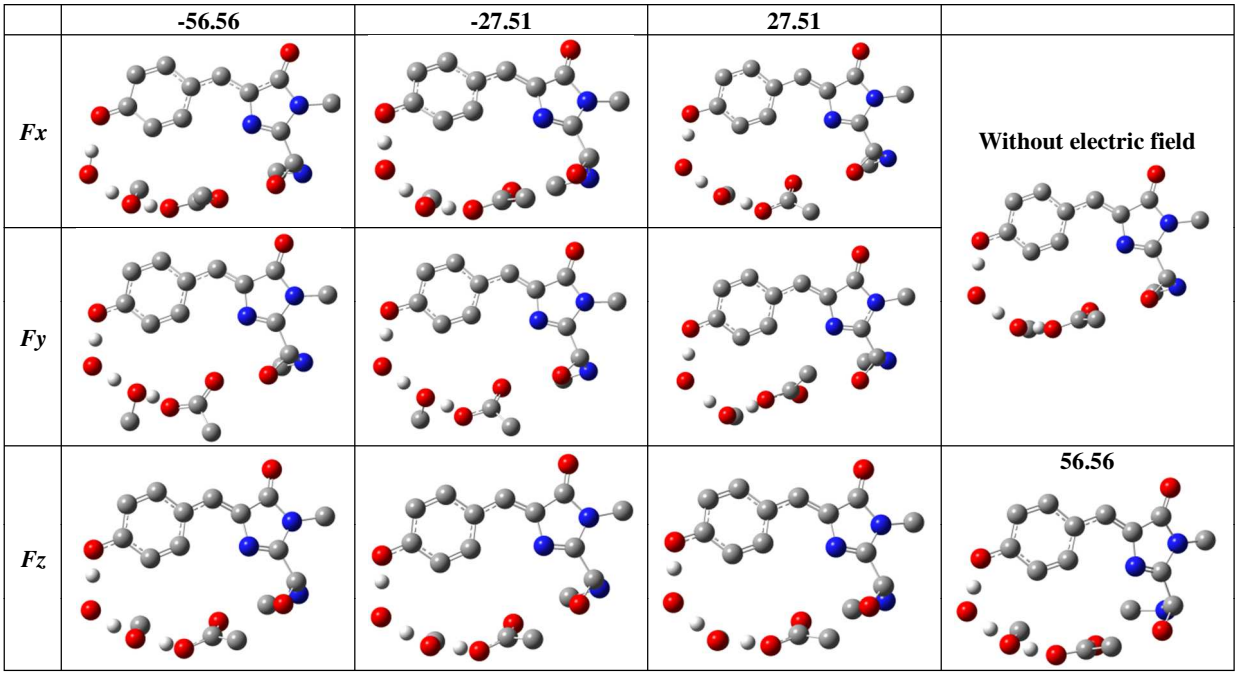

Figure 4. Optimized structures of transition states under the influence of electric fields. To clearly show the protons motions, only the transferred three protons are drawn.

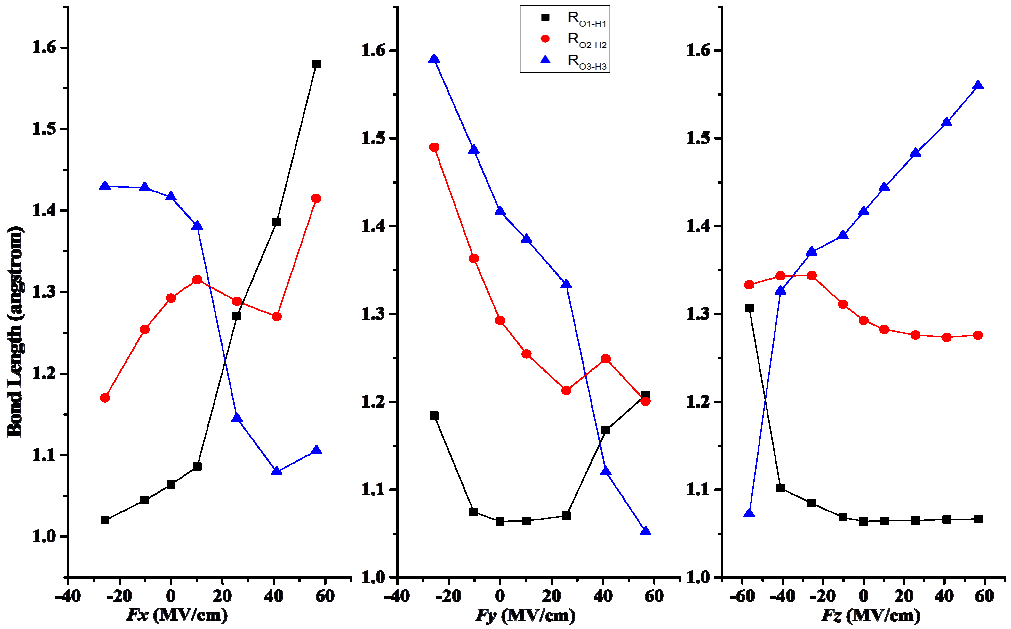

Figure 5. OH bond lengths changes vs. electric fields

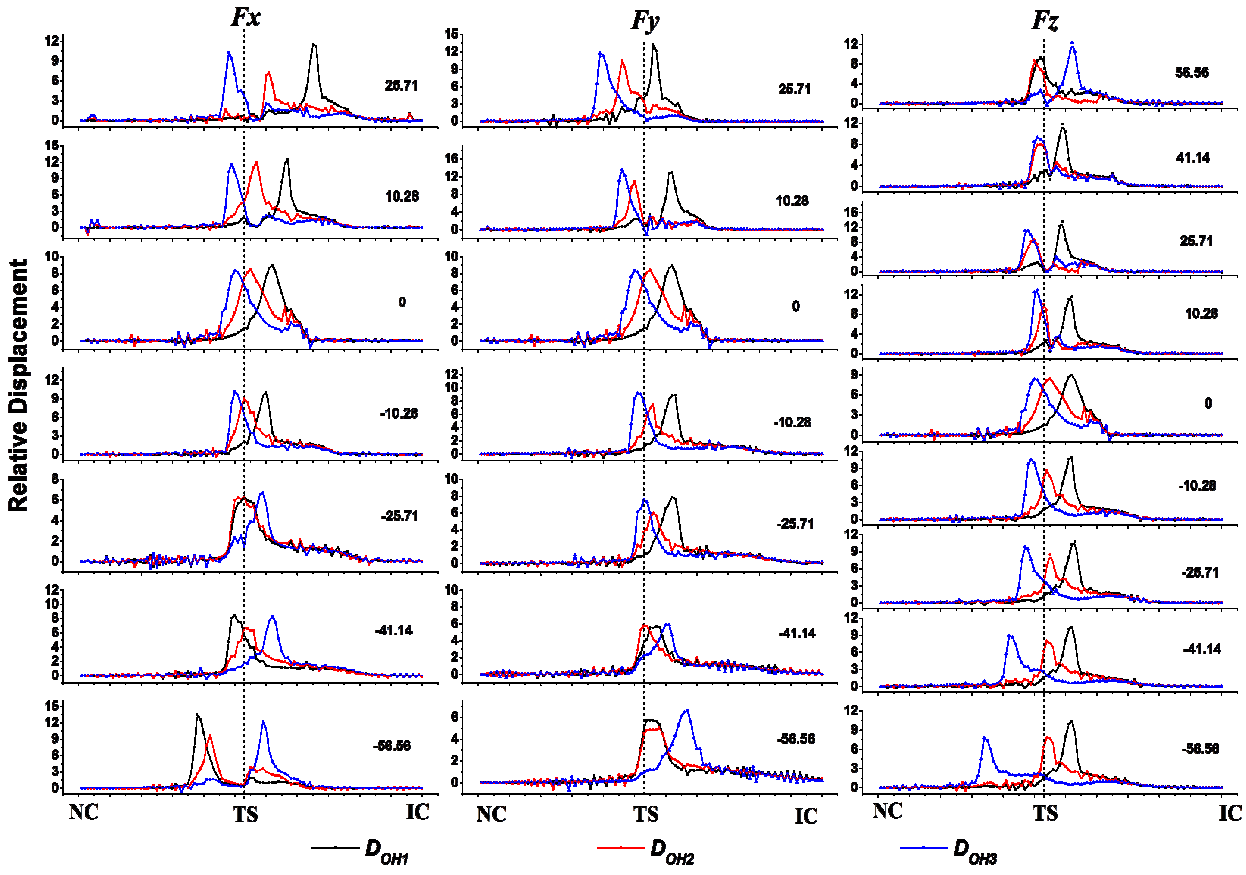

Figure 6. Relative displacements of protons under the influence of electric fields

modulate the proton transfer mechanism.

As can be seen from Figure 1, ***Fx***, ***Fy*** and ***Fz*** all obviously change the PES shapes, but with different tendency.

When Fx gradually increases from -56.56 MV/cm to 25.71 MV/cm, IC becomes more energetically stable with much reduced $\Delta G^{\ddagger}$. Whereas, from negative to positive, ***Fy*** and ***Fz*** turn out to favor NC in energy and progressively increases ΔG‡. This phenomenon can be further verified by the equilibrium constant (***K***) changes upon electric fields. Once the $\Delta G^{\ddagger}$ and ΔE were acquired, the forward and backward reaction rates (k_1 and k_2) can be computed by CTST equation. As demonstrated in Figure 2, surprisingly the electric field effect on the magnitude of ***K (log K)*** can be closely fitted to a linear relationship for each orientation. Furthermore, it can be classified into two categories, ***Fx*** and ***Fy&Fz***, based on the slopes of fitted lines. This difference should originate from the dipole moment direction of the complex (in Figure 3). For IC, the ***x*** component of dipole moment is negative, while the ***y*** and ***z*** ones are positive (all the energy values are based on NC). It is noteworthy that barrierless reaction can take place under certain conditions (at ***Fx***+27.71 and ***Fy***+25.71). From this point, ***Fx*** and ***Fy*** have stronger effect on the PES than ***Fz***, which can be also evidenced by the absolute values of slopes in Figure 2. Moreover, the electric field can control the reaction rate from picosecond to second in time scale as listed in Table 1. Additionally, we investigated the effect of continuum solvent field on PES by polarizable continuum model (PCM) calculations. However, the results exhibit that solvent effect has little effect on PES.

For the TS in electric field free, protons give a sequential motion as displayed in Figure 4. H1 still resides on the phenol ring, with bond length of O1-H1 ($R_{O1\text{-}H1}$) slightly increasing to 1.064 Å. H3 has migrated from O3 and almost bonded to O4 with bond length of H3-O4 ($R_{H3\text{-}O4}$) of 1.070 Å. In the meantime, H2 is in the process of moving across from O2 to O3, with bond lengths of O2-H2 and H2-O3 ($R_{O2\text{-}H2}$ and $R_{H2\text{-}O3}$) of 1.292 Å and 1.134 Å. To further explore the proton transfer mechanism, the relative displacement of each proton (D_{OH}) at given point along the reaction coordinates was investigated, which was defined by Wang *et al*[51] and expressed as:

$$D_{OH} = \frac{b_{i+1} - b_i}{\frac{1}{n}\sum_{i=1}^{n}(b_{i+1} - b_i)}$$

where the b_{i+1} and b_i are the OH distances along the reaction coordinate. From Figure 5, the GSPT shows an asynchronous character without electric field. Including the single barrier, the GSPT reaction should be a concerted and asynchronous process which has been stated in our early study.[52] It needs to be emphasized that GSPT is concerted process regardless of electric field, owing to the single barrier along PES (for ***Fx***+25.71 and ***Fy***+25.71, the GSPT is barrierless process. If without ZPE, all the PESs have single barrier). It was further revealed no intermediates exist through IRC calculations and TSs are real transition states with only one imaginary vibrational mode from the frequency calculations. Electric fields strongly affect the TS

Table 2. Detailed absorption properties including electric fields by TDDFT method

		NC			IC		
F		λ (nm)	Oscillator Strength	Orbital Transition	λ (nm)	Oscillator strength	Orbital Transition
x	**56.56**	340.6	0.5558	H→L+1 (72.1%)	354.3	0.0037	H→L (79.5%)
	41.14	333.2	0.7198	H→L (96.1%)	355.1	0.8665	H→L (100%)
	25.71	335.4	0.6399	H→L (96.6%)	368.3	0.9050	H→L (100%)
	10.28	338.8	0.7229	H→L (100%)	382.2	0.9288	H→L (100%)
	0	344.6	0.7241	H→L (100%)	391.0	0.9403	H→L (100%)
	-10.28	350.9	0.7631	H→L (100%)	398.6	0.9358	H→L(95.3%)
	-25.71	360.8	0.8010	H→L (88.1%)	406.6	0.8525	H→L+1(68.1%)
	-41.14	372.1	0.8194	H→L+1(91.3%)	519.71	0.0088	H→L (97.5%)
	-56.56	469.0	0.0092	H→L (97%)	797.06	0.0034	H→L (97.3%)
y	**56.56**	337.7	0.649	H→L+2 (70.0%)	468.6	0.0036	H→L (100%)
	41.14	337.9	0.6687	H→L (94.6%)	394.5	0.8079	H→L+3 (59.5%)
	25.71	340.3	0.6779	H→L (100%)	390.72	0.8947	H→L (78.2%)
	10.28	343.9	0.6913	H→L (100%)	391.13	0.9159	H→L (97.9%)
	0	344.6	0.7241	H→L (100%)	391.0	0.9403	H→L (100%)
	-10.28	346.5	0.7659	H→L (100%)	391.29	0.9590	H→L (100%)
	-25.71	349.6	0.7598	H→L (100%)	392.69	0.9866	H→L (100%)
	-41.14	357.6	0.7630	H→L (80.4%)	394.63	0.9826	H→L (100%)
	-56.56	371.6	0.0441	H→L+1(51.2%)	439.64	0.0033	H→L (100%)
z	**56.56**	342.9	0.7208	H→L (100%)	399.44	0.003	H→L (97.6%)
	41.14	342.4	0.7240	H→L (100%)	391.98	0.9127	H→L+1(54.2%)
	25.71	342.3	0.7282	H→L (100%)	391.68	0.920	H→L (100%)
	10.28	343.7	0.7269	H→L (100%)	391.85	0.9241	H→L (100%)
	0	344.6	0.7241	H→L (100%)	391.0	0.9403	H→L (100%)
	-10.28	344.6	0.7641	H→L (100%)	390.92	0.9462	H→L (100%)
	-25.71	345.4	0.7632	H→L (100%)	391.37	0.9501	H→L (100%)
	-41.14	347.8	0.7620	H→L (100%)	392.23	0.9483	H→L+1(100%)
	-56.56	350.2	0.7312	H→L (100%)	394.39	0.8862	H→L+1(89.7%)

structures (in Figure 4), which can also be evidenced by the OH bond lengths changes displayed in Figure 5. At ***Fx***+25.71, H1 still stays at the phenol side with slightly decreased $R_{O1\text{-}H1}$ of 1.020 Å, H3 moves to O4 with shorted $R_{H3\text{-}O4}$ of 1.068 Å, H2 still in the process from O2 to O3. That is, it retains the proton transfer ordering with H3 to be first and H1 to be the last to move, and the asynchronism is enhanced as evidenced by the D_{OH} in Figure 6. When negative ***Fx*** was applied, $R_{O1\text{-}H1}$ increases and $R_{O3\text{-}H3}$ decreases. At ***Fx***-56.56, $R_{O1\text{-}H1}$ much increases to 1.580 Å, implying H1 has migrated to O2. At the same time, $R_{H3\text{-}O3}$ significantly reduces to 1.101 Å, that is, H3 turns out to reside in acetate side. It reflects the proton transfer ordering change that H1 appears to be the first and H3 is the last to move, which is opposite to the case without electric field. Similar phenomenon was observed for ***Fy*** and ***Fz*** as well, while the trends of ***Fz*** is different from that of ***Fx*** and ***Fy***.

Then TDDFT calculations were performed to systematically investigate the electric field effects on the photochemical properties of the H-bonded HBDI complex. Without electric field, the first excitation energies of NC (λ_{NC}) and IC (λ_{IC}) were calculated to be 345 nm and 391 nm, both corresponding to the HOMO to LUMO transition (H→L). When the electric fields were explored, as listed in Table 2, the first excitations in most cases still correspond to the H→L transition. But some cases turn to be H→L+1 transition or even H→L+2 transition, which should be introduced by the orbital distortions by strong electric field. Furthermore, one can clearly see that LUMO shape significantly changes under very strong field as seen in Supplementary Material (Figure S2). As we expected, absorption energies obtained by TDDFT are more acceptable than HOMO-LUMO gap.

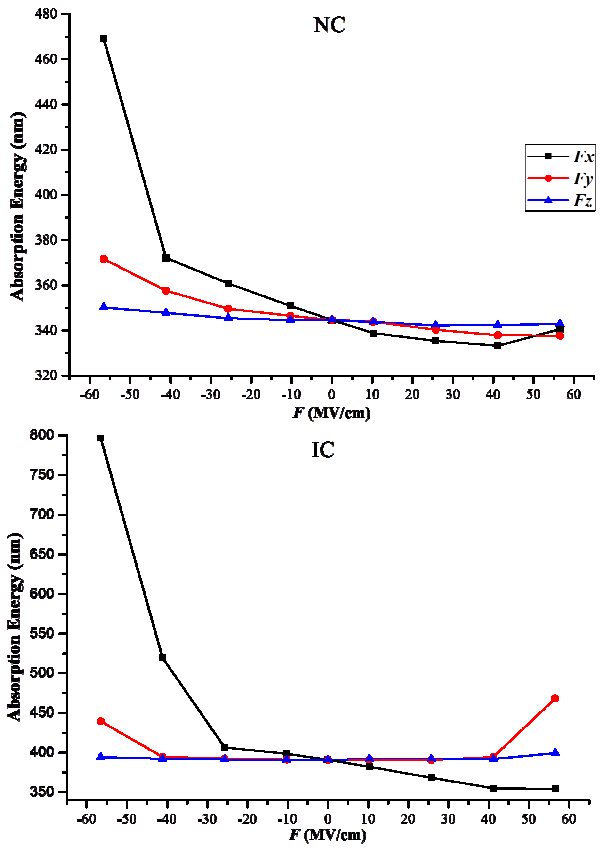

Figure 7. Absorption energies of NC and IC upon the

The absorption wavelength (λ_{NC} for NC and λ_{IC} for IC) changes upon electric fields were depicted in Figure 7. It is clear that ***Fx*** has the largest effect and ***Fz*** has the smallest effect on both λ_{NC} and λ_{IC}. The $\lambda_{NC}/\lambda_{IC}$ is much blue-shifted from 469/797nm at ***Fx***-56.56 MV/cm to 341/354 nm at ***Fx***+56.56 MV/cm. Under the effect of ***Fy***, the $\lambda_{NC}/\lambda_{IC}$ changes by about 35/75 nm, which is much smaller than that under ***Fx.*** Both the λ_{NC} and λ_{IC} change within 10 nm under ***Fz***. The much larger sensitivity of λ_{NC} and λ_{IC} to ***Fx*** should originate from the charge transfer state between imidazolium and phenol, *i.e.* ***x*** direction, during excitation.[40, 42] It should be noticed, in ref. 26, the sensitivity of λ_{IC} to ***Fy*** is almost comparable to that to ***Fx***, which is different from our results. This is sourced from the simple HOMO-LUMO gap treatment in ref. 26. Furthermore, λ_{IC} is more sensitive to electric field than λ_{NC}, which is in good agreement with experimental observation that anionic form is more sensitive to environments.[53]

Conclusions

In summary, we presented DFT calculations to understand electric field effects on GSPT process in the H-bonded HBDI complex, which can represent the active site of GFP. The PESs in the absence or presence of electric field were purchased. Electric fields show significant influence on the shapes of PESs. They can be classified into two groups, ***Fx*** and ***Fy*** & ***Fz,*** based on the effect on magnitude of ***K***. From negative to positive, *Fx* favors NC in energy while ***Fy*** & ***Fz*** prefers IC to be the dominating conformer, which should originate from the dipole moment orientation of IC. Furthermore, the electric field effects on log ***K*** can be closely fitted to a linear relationship. It was revealed that GSPT should be concerted process, no matter electric fields were applied or not, due to only one barrier and no intermediates existing. However, the proton motions including the ordering and synchronism can be strongly affected by the electric fields as evidenced by the relative displacements of protons. In addition, electric field appears to be a possible method to manipulate the absorption energies and ***Fx*** has the largest effect than the other two because of the charger transfer along *x* axis during photo-excitation. Moreover, IC is found to be more sensitive to electric filed than NC. Our results are helpful to understand the HBDI behaviors under the electric fields and can be used for rational design of the FPs with desirable conformer and absorption energy by site directed mutagenesis. Undoubtedly, we will extend our effort on this issue and hope to dig deeper insight.

Acknowledge

This work was supported by National Research Foundation (NRF) grants funded by the Korean government (MEST) (2007-0056343) and (2011-0015767). We acknowledge the financial support from the Ministry of Education, Science and Technology, subjected to the project EDISON (Education-research Integration through Simulation On the Net, Grant No.: 2012M3C1A6035359). The authors would like to acknowledge the support from KISTI

supercomputing center through the strategic support program for the supercomputing application research [No. KSC-2012-C3-25].

Notes and references

[a] *Department of Chemistry, Sungkyunkwan University, Suwon, 440746, Korea*
[b] *Department of Chemistry, Seoul National University, Seoul 151-742, Korea.*

1. M. Zimmer, *Chem. Rev.* , 2002, **102**, 759-781.
2. V. I. Martynov and A. A. Pakhomov, *Chem. Biol.*, 2008, **15**, 755-764.
3. B. N. G. Giepmans, S. R. Adams, M. H. Ellisman and R. Y. Tsien, *Science*, 2006, **312**, 217-224.
4. M. Zimmer, *Chem. Soc. Rev.* , 2009, **38**, 2823-2832.
5. R. Hein and R. Y. Tsien, *Curr. Biol.*, 1996, **6**, 178-182.
6. H. Morise, O. Shimomura, F. H. Johnson and J. Winant, *Biochemistry-Us*, 1974, **13**, 2656-2662.
7. W. W. Ward and S. H. Bokman, *Biochemistry-Us*, 1982, **21**, 4535-4540.
8. S. Boye, H. Krogh, I. B. Nielsen, S. B. Nielsen, S. U. Pedersen, U. V. Pedersen, L. H. Andersen, A. F. Bell, X. He and P. J. Tonge, *Phys. Rev. Lett.* , 2003, **90**.
9. I. V. Yampolsky, S. J. Remington, V. I. Martynov, V. K. Potapov, S. Lukyanov and K. A. Lukyanov, *Biochemistry-Us*, 2005, **44**, 5788-5793.
10. K. Brejc, T. K. Sixma, P. A. Kitts, S. R. Kain, R. Y. Tsien, M. Ormo and S. J. Remington, *P. Natl. Acad. Sci. USA.*, 1997, **94**, 2306-2311.
11. M. Ormo, A. B. Cubitt, K. Kallio, L. A. Gross, R. Y. Tsien and S. J. Remington, *Science*, 1996, **273**, 1392-1395.
12. R. Bizzarri, M. Serresi, S. Luin and F. Beltram, *Anal. Bioanal.Chem.* , 2009, **393**, 1107-1122.
13. T. B. McAnaney, E. S. Park, G. T. Hanson, S. J. Remington and S. G. Boxer, *Biochemistry-Us*, 2002, **41**, 15489-15494.
14. A. B. Cubitt, L. A. Woollenweber and R. Heim, *Method. Cell Biol.*, 1999, **58**, 19-+.
15. M. P. Lesser, F. Bou-Abdallah and N. D. Chasteen, *Bba-Gen. Subjects*, 2006, **1760**, 1690-1695.
16. F. Yang, L. G. Moss and G. N. Phillips, *Nat. Biotechnol.* , 1996, **14**, 1246-1251.
17. M. F. Perutz, *Science*, 1978, **201**, 1187-1191.
18. A. WARSHEL, *Acc. Chem. Res.* , 1981, **14**, 284-299.
19. K. A. Sharp and B. Honig, *Annu. Rev. Biophys. Biophys. Chem.*, 1990, **19**, 301-332.
20. P. R. Callis and B. K. Burgess, *J. Phys. Chem. B* 1997, **101**, 9429-9432.
21. E. S. Park, S. S. Andrews, R. B. Hu and S. G. Boxer, *J. Phys. Chem. B* 1999, **103**, 9813-9817.
22. J. M. Kriegl, K. Nienhaus, P. C. Deng, J. Fuchs and G. U. Nienhaus, *P. Natl. Acad. Sci. USA.*, 2003, **100**, 7069-7074.
23. T. Nakabayashi, M. Kinjo and N. Ohta, *Chem. Phys. Lett.* , 2008, **457**, 408-412.
24. T. Ito, S. Oshita, T. Nakabayashi, F. Sun, M. Kinjo and N. Ohta, *Photoch. Photobiol. Sci.*, 2009, **8**, 763-767.
25. T. Nakabayashi, K. Hino, Y. Ohta, S. Ito, H. Nakano and N. Ohta, *J. Phys. Chem. B* 2011, **115**, 8622-8626.
26. I. Topol, J. Collins, A. Savitsky and A. Nemukhin, *Biophys. Chem.* , 2011, **158**, 91-95.
27. H. J. Kreuzer, *Surf. Interface Anal.* , 2004, **36**, 372-379.
28. A. D. Bandrauk, E. W. S. Sedik and C. F. Matta, *J. Chem. Phys.* , 2004, **121**, 7764-7775.
29. A. D. Bandrauk, E. S. Sedik and C. F. Matta, *Mol. Phys.* , 2006, **104**, 95-102.
30. A. A. Arabi and C. F. Matta, *Phys. Chem. Chem. Phys.* , 2011, **13**, 13738-13748.
31. W. Weber, V. Helms, J. A. McCammon and P. W. Langhoff, *P. Natl. Acad. Sci. USA.*, 1999, **96**, 6177-6182.
32. M. Chattoraj, B. A. King, G. U. Bublitz and S. G. Boxer, *P. Natl. Acad. Sci. USA.*, 1996, **93**, 8362-8367.
33. A. Warren and M. Zimmer, *J. Mol. Graph Model.*, 2001, **19**, 297-303.
34. R. Yam, E. Nachliel, S. Kiryati, M. Gutman and D. Huppert*, *Biophys. J.* , 1991, **59**, 4-11.
35. N. Muzet, B. Guillot, C. Jelsch, E. Howard and C. Lecomte, *P. Natl. Acad. Sci. USA.*, 2003, **100**, 8742-8747.
36. J. Y. Hasegawa, K. Fujimoto, B. Swerts, T. Miyahara and H. Nakatsuji, *J. Comput. Chem.* , 2007, **28**, 2443-2452.
37. S. F. Wang and S. C. Smith, *Phys. Chem. Chem. Phys.* , 2007, **9**, 452-458.
38. H. Zhang, Q. Sun, Z. Li, S. Nanbu and S. S. Smith, *Comput. Theor. Chem.*, 2012, **990**, 185-193.
39. O. Vendrell, R. Gelabert, M. Moreno and J. M. Lluch, *J. Am. Chem. Soc.* , 2006, **128**, 3564-3574.
40. X. Li, L. W. Chung, H. Mizuno, A. Miyawaki and K. Morokuma, *J. Phys. Chem. B* 2010, **114**, 1114-1126.
41. M. J. Frisch, G. W. Trucks, H. B. Schlegel, G. E. Scuseria, M. A. Robb, J. R. Cheeseman, G. Scalmani, V. Barone, B. Mennucci, G. A. Petersson, H. Nakatsuji, M. Caricato, X. Li, H. P. Hratchian, A. F. Izmaylov, J. Bloino, G. Zheng, J. L. Sonnenberg, M. Hada, M. Ehara, K. Toyota, R. Fukuda, J. Hasegawa, M. Ishida, T. Nakajima, Y. Honda, O. Kitao, H. Nakai, T. Vreven, J. A. Montgomery, Jr., J. E. Peralta, F. Ogliaro, M. Bearpark, J. J. Heyd, E. Brothers, K. N. Kudin, V. N. Staroverov, T. Keith, R. Kobayashi, J. Normand, K. Raghavachari, A. Rendell, J. C. Burant, S. S. Iyengar, J. Tomasi, M. Cossi, N. Rega, J. M. Millam, M. Klene, J. E. Knox, J. B. Cross, V. Bakken, C. Adamo, J. Jaramillo, R. Gomperts, R. E. Stratmann, O. Yazyev, A. J. Austin, R. Cammi, C. Pomelli, J. W. Ochterski, R. L. Martin, K. Morokuma, V. G. Zakrzewski, G. A. Voth, P. Salvador, J. J. Dannenberg, S. Dapprich, A. D. Daniels, O. Farkas, J. B. Foresman, J. V. Ortiz, J. Cioslowski and D. J. Fox, Gaussian 09, Revision B.01, Gaussian, Inc., Wallingford CT, 2010.
42. J. M. G. de la Vega and B. Miguel, *Theor. Chem. Acc.* , 2000, **104**, 189-194.
43. T. Yanai, D. P. Tew and N. C. Handy, *Chem. Phys. Lett.* , 2004, **393**, 51-57.
44. A. Zawada, A. Kaczmarek-Kedziera and W. Bartkowiak, *J. Mol. Model.* , 2012, **18**, 3073-3086.
45. R. F. Li, J. J. Zheng and D. G. Truhlar, *Phys. Chem. Chem. Phys.*, 2010, **12**, 12697-12701.
46. R. Kobayashi and R. D. Amos, *Chem. Phys. Lett.* , 2006, **424**, 225-225.
47. R. Kobayashi and R. D. Amos, *Chem. Phys. Lett.* , 2006, **420**, 106-109.
48. K. Raghavachari, g. W. Trucks, j. A. Pople and m. Head-gordon, *Chem. Phys. Lett.* , 1989, **157**, 479-483.
49. D. G. Truhlar, B. C. Garrett and S. J. Klippenstein, *J. Phys. Chem* , 1996, **100**, 12771-12800.
50. K. Winkler, J. R. Lindner, V. Subramaniam, T. M. Jovin and P. Vohringer, *Phys. Chem. Chem. Phys.*, 2002, **4**, 1072-1081.
51. S. F. Wang and S. C. Smith, *J. Phys. Chem. B* 2006, **110**, 5084-5093.
52. B. Kang, S. Karthikeyan, D.-J. Jang, H. Kim and J. Y. Lee, *Bull. Korean Chem. Soc.* , 2013, **34**, 1961 - 1966.
53. J. Dong, K. M. Solntsev and L. M. Tolbert, *J. Am. Chem. Soc.*, 2006, **128**, 12038-12039.

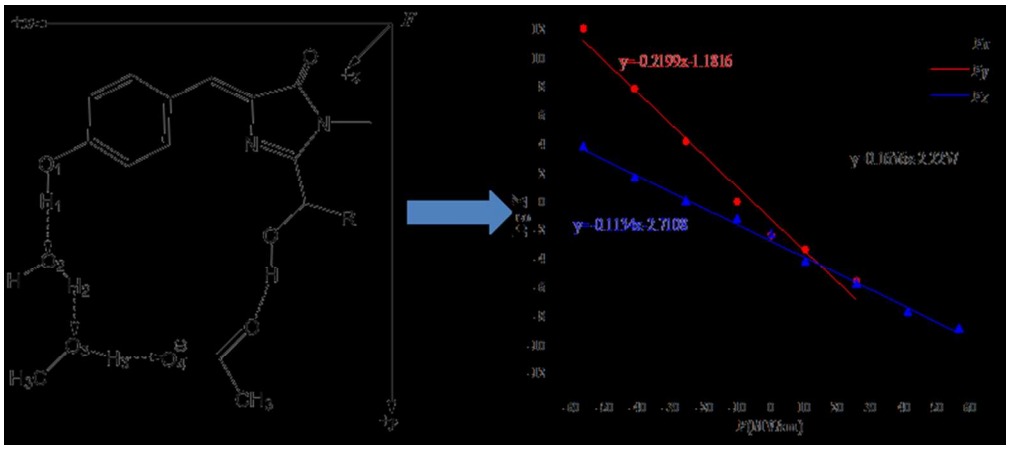

134x58mm (150 x 150 DPI)